Cancer Science
The official journal of the Japanese Cancer Association

Role of syndecan-1 (CD138) in cell survival of human urothelial carcinoma

Keiji Shimada,[1] Mitsutoshi Nakamura,[1] Marco A. De Velasco,[2] Motoyoshi Tanaka,[2] Yukiteru Ouji,[3] Makito Miyake,[4] Kiyohide Fujimoto,[4] Kazuya Hirao[5] and Noboru Konishi[1,6]

[1]Department of Pathology, Nara Medical University School of Medicine, Nara; [2]Department of Urology, Kinki University School of Medicine, Osaka; Departments of [3]Parasitology, [4]Urology, Nara Medical University School of Medicine, Nara; [5]Department of Urology, Hirao Hospital, Nara, Japan

(Received July 29, 2009/Revised September 7, 2009/Accepted September 16, 2009/Online publication October 26, 2009)

Heparan sulfate proteoglycan syndecan-1, CD138, is well known to be associated with cell proliferation, adhesion, and migration in various types of malignancies. In the present study, we focused on the role of syndecan-1 in human urothelial carcinoma of the urinary bladder. Silencing of syndecan-1 by siRNA transfection down-regulated transcriptional factor junB and the long isoform of FLICE-inhibitory protein (FLIP long), resulting in the induction of apoptosis in the urothelial carcinoma cell lines UMUC2 and UMUC3. Knockdown of junB and FLIP long as well as syndecan-1 silencing mediated apoptosis that was inhibited by pan-caspase inhibitors. Transurethral injection of syndecan-1 siRNA into the urinary bladder significantly reduced syndecan-1 gene expression and growth of red fluorescent-labeled KU-7/RFP bladder cancer cells in the mouse orthotopic bladder cancer model. Immunohistochemical examination showed high syndecan-1 protein expression in high-grade, superficial, and deep invasive carcinomas (pT1 and ≥pT2) as well as carcinoma *in situ,* but not in low-grade and non-invasive phenotypes (pTa). In addition, the percentage of cancer cells positive for syndecan-1 at initial diagnosis was statistically associated with the frequency of bladder cancer recurrence after transurethral resection. In conclusion, syndecan-1 might contribute to urothelial carcinoma cell survival and progression; therefore, this molecule could be a new therapeutic target in human urinary bladder cancer. (*Cancer Sci* 2010; 101: 155–160)

Syndecan-1 (CD138), a member of four mammalian heparin sulfate proteoglycans, is highly expressed in many types of normal epithelilal cells and malignant counterparts where it plays an important role in cell growth, adhesion, migration, epithelial morphogenesis, and angiogenesis.[1] Syndecan-1 is over-expressed in normal and malignant plasma cells, contributing to plasma cell myeloma development [2,3]: heparin sulfate-epidermal growth factor-ligands were shown to be concentrated by syndecan-1 at the cell membrane, resulting in activation of ErbB-meditaed cell survival signals.[4] Derksen *et al.* reported that syndecan-1 functions as a coreceptor for hepatocyte growth factor (HGF) and promotes myeloma cell proliferation.[5] Of note, treatment with an inhibitor of human heparanase, an enzyme that synergizes with syndecan-1 in promoting myeloma progression, or knockdown of syndecan-1 expression by RNAi diminished myeloma tumor development *in vivo*.[6] In addition to hematopoietic malignancies, the soluble and membrane-bound forms of syndecan-1 could enhance breast cancer progression: proteolytic conversion of Sdc1 from being membrane-bound into a soluble molecule marks a switch from a proliferative to an invasive phenotype.[7] We have previously demonstrated that syndecan-1 participates in the process of androgen-dependent to -independent conversion, and be a new target molecule for hormone-resistant prostate cancer therapy.[8] Thus, syndecan-1 plays important roles in not only hematopoietic but also epithelial tumor development.

A variety of cells progress to a malignant phenotype through accumulation of genetic and epigenetic abnormalities in key signals that regulate cell growth, survival, cell death, or cell-to-cell interaction.[9] Urothelial carcinomas appear to be grouped into two types, markedly differing in their biological behavior and prognoses: low-grade (G1, G2)/noninvasive cancers (pTa, pT1), including papillary urothelial neoplasms of low malignant potential, and high-grade (G3)/muscle invasive lesions (greater than pT2). Approximately 80% of urothelial carcinomas are of the noninvasive type, these often being multifocal or recurrent (~70%) but with limited muscle invasion (~15%) and good prognosis.[10] This type of tumor harbors frequent mutations in *ras* (30–40%) and fibroblast growth factor receptor 3 (~70%) genes,[11,12] suggesting primary involvement of the activation of receptor tyrosine kinase and oncogenic *ras*. In contrast, high-grade and muscle invasive cancers progress to local and distant metastases. They seem to arise de novo or from high-grade carcinoma *in situ* and show loss of function of the tumor suppressor genes *p53* and/or *Rb*.[13] Our recent research identified c-jun NH2 terminal kinase or human AlkB human homologue-8 (ALKBH-8) as a novel signal required for invasive urothelial carcinomas.[8,14] Syndecan-1 has been reported to be highly expressed in plasamcytoid urothelial carcinoma which is considered to be an aggressive phenotype,[15–17] demonstrating that syndecan-1 is closely associated with urothelial carcinoma progression. In the current study, we studied the molecular mechanisms by which syndecan-1 affects survival signals in human urothelial carcinoma cells *in vitro* and *in vivo*; moreover, we examined the clinical relevance by performing immunohistochemical analysis from human bladder cancer specimens. Knockdown of syndecan-1 induced apoptosis by down-regulating the transcriptional factor junB and FLIP, resulting in caspase activation *in vitro*. Interestingly, transurethral injection of siRNA into the urinary bladder with atelocollagen successfully reduced expression of the syndecan-1 gene *in vivo* and reduced bladder cancer growth in the mouse orthotopic bladder cancer model.

Materials and Methods

Cell culture, plasmids, and chemicals. Human urothelial carcinoma cell lines UMUC2 and UMUC3 were cultured in RPMI supplemented with 10% fetal bovine serum. The origins of UMUC2 and UMUC3 are ureteral tumor (carcinoma *in situ*) and bladder tumor (invaded carcinoma), respectively. Wild type of p53 is observed in UMUC2 cells, but it is largely deleted in UMUC3 cells. [18] Anti-poly (ADP-ribose) polymerase (PARP), anti-FLIP (long and short isoforms), anto-Fas, anti-Fas associated death domain protein (FADD), anti-caspase 8, and anti-junB antibodies were purchased from Cell Signaling (Boston, MA, USA); anti-actin antibody was from Santa Cruz Biotechnology

[6]To whom correspondence should be addressed.
E-mail: nkonishi@naramed-u.ac.jp

doi: 10.1111/j.1349-7006.2009.01379.x

(Santa Cruz, CA, USA); and anti-syndecan-1 (CD138) antibody was from Dako Japan (Tokyo, Japan).

Preparation of cell lysates and Western blotting analysis. Cell lysates were resolved in SDS-polyacrylamide gels and transferred to polyvinylidene difluoride membranes (Millipore, Billerica, MA, USA) that were then blocked in 5% skim milk at room temperature for 1 h. Membranes were incubated with the indicated primary antibody for 1 h, and then incubated with horseradish peroxidase–conjugated antimouse or antirabbit IgG (Amersham Pharmacia, London, UK). Peroxidase activity on was detected on X-ray film using an enhanced chemiluminescence detection system.

Reverse-transcription PCR. Using the One-step RT-PCR kit (Qiagen Japan, Tokyo, Japan), we extracted total RNA using Trizol reagent and subjected it to reverse-transcription PCR (RT-PCR). PCR conditions were 95°C for 30 s, 55–60°C for 30 s, and 72°C for 1 min through a total of 30 cycles. The PCR primer sequences for syndecan-1 were: 5′-GGCTGTAGTCCTGCCAGAAG-3′ (sense) and 5′-GTTGAGGCCTGATGAGTGGT-3′ (antisense). The primers for junB were 5′-ACTCATACACAGCTACGGGATACG-3′ (sense) and 5′-GGCTCGGTTTCAGGAGTTTG-3′ (antisense). The primers for FLIP long isoform were 5′-CTGCTCTACAGAGTGAGGCG-3′ (sense) and 5′-AAACAAGGTGAGGGTTCCTG-3′ (antisense). The primers for FLIP short isoform were 5′-CTGCTCTACAGAGTGAGGCG-3′ (sense) and 5′-AAACAAGGTGAGGGTTCCTG-3′ (antisense). For glyceraldehyde-3-phosphate dehydrogenase (G3PDH), the primers used were 5′-ACCACAGTCCATGCCATCAC-3′ (sense) and 5′-TCCACCACCCTGTTGCTGTA-3′ (antisense).

siRNA transfection of syndecan-1, junB or FLIP long isoform. For transfection analyses, 10^6 cells from each urothelial carcinoma were seeded in 6-cm dish plates and transfected with either 100 nM of control RNA (Santa Cruz Biotechnology) or with the siRNA of syndecan-1 or NOX2. Transfections were carried out using the Lipofectamine system (Invitrogen Japan, Tokyo, Japan) in accordance with the manufacturer's protocol. The syndecan-1 siRNA duplexes, generated with 3′-dTdT overhangs and prepared by Qiagen, were chosen against the DNA target sequences as follows: 5′-CACCATTCTGACTCGGTTTCT-3′. The junB siRNA duplexes, generated with 3′-dTdT overhangs and prepared by Qiagen, were chosen against the DNA target sequences as follows: 5′-CACGACTACAAACTCCTGAAA-3′. The FLIP siRNA was purchased from Santa Cruz Biotechnology.

Terminal deoxynucleotidyl transferase-mediated dUTP nick end labeling (TUNEL) assay. Formalin-fixed and paraffin-embedded 5-μm-thick sections of all tumor samples were used to identify apoptotic cells by TUNEL staining using the tumor TACS *in situ* apoptosis detection kit (R&D Systems, Minneapolis, MN, USA). The apoptotic index (per ×400 microscopic field) was calculated as the number of apoptotic cells × 100 per total number of cells.

Cell proliferation assay. Cells were stimulated with various reagents for a given period, after which MTS reagent (3-(4,5-dimethylthiazol-2-yl)-5-(3-carboxymethoxyphenyl)-2-(4-sulphonyl)-2H-tetrazolium, inner salt (Promega, Tokyo, Japan) was added. After a 3-h incubation period, optical absorbance at 490 nm was measured using a microplate reader. Cell viability was expressed as mean ratio with SDs of absorbance after control RNA and syndecan-1 siRNA transfections. All experiments were performed in triplicate.

Apoptosis detection assay. After transfections with siRNA, cells were collected and stained with propidium iodide (PI) and FITC-conjugated Annexin V (AV) according to the manufacturer's protocol (TACS Annexin V-FITC kit; R&D Systems). Then, cells undergoing apoptosis were quantified by counting the number of cells with bound AV but negative for PI. All experiments were performed at least three times in duplicate.

Tissue samples and immunohistochemistry. We obtained human urinary bladder cancer specimens, diagnosed as urothelial carcinomas ($n = 51$), from patients undergoing transurethral resection or radical cystectomy, without previous radiation or chemotherapy, at Nara Medical University Hospital, Japan. Clinicopathological data of the present cases are summarized in Table 1 according to the grading and staging of the 2004 World Health Organization classification. Informed consent was obtained from all patients before the collection of specimens, as appropriate, and tumor stage and grade were noted at the time of diagnosis. We followed the same tissue fixation and processing procedure as described in a previous report.[8,19,20]

Construction of KU-7 stably expressing RFP. KU-7, a human bladder cancer cell line, was derived from a low-grade and superficial papillary tumor. However, KU-7 cells can rapidly grow and invade into the subepithelial stromal tissues after inoculation into the urinary bladder of nude mice. KU-7 cells were maintained in Gibco DMEM (Invitrogen, Carlsbad, CA, USA) supplemented with 10% fetal calf serum in a 37°C incubator with 5% CO_2. Stable fluorescent tumor cell lines were generated by transfection with pDsRed-N1 vectors (Clonetech, Palo Alto, CA, USA) by using Fugene 6 transfection reagent (Roche, Indianapolis, IN, USA) according to the manufacturer's protocol. Cells were harvested by trypsin/EDTA 48 h after transfection and subcultured into selective medium in the presence of G418. Stable clones expressing high level of red fluorescence protein (RFP) were used and designated KU-7/RFP.

Orthotropic implantation model. Eight-week-old female nude mice were maintained and used for our experiments.[14] The mice were purchased from CLEA (Tokyo, Japan) and the diet was CLEA Rodent Diet (http://www.clea-japan.com/Feed/cl2.html). Seven days after transcatheter inoculation of 5×10^7 KU-7 cells expressing RFP into the urinary bladder, mice were randomized into a control (control RNA + atelocollagen, $n = 10$) or syndecan-1 knockdown (syndecan-1 siRNA + atelocollagen, $n = 9$) treatment group and received a single intravesical treatment instillation that was retained for 1 h by purse-string suture. Mice were sacrificed 7 days after treatment and bladders were removed, splayed open on filter paper, and fixed in 10% neutral buffered formalin. Tumor burden was determined by analyzing images of RFP fluorescence from tumor cells on flat formalin-fixed bladders captured using a macro-imaging station consisting of a SBIG cooled CCD camera model ST-7XME (Santa Barbara Imaging Group, Santa Barbara, CA, USA) mounted onto a dark box. Bladders were embedded in paraffin, step-sectioned, and stained with hematoxylin–eosin (H&E). Results from animal experiments were compiled from data generated from three independent experiments as previously demonstrated.[8,21]

Image analysis. Image analysis was performed with ImageJ public domain software available through the National Institutes

Table 1. Characterization of urothelial carcinomas

Age (years)	71.1 (44–96)
Gender (M:F)	40:11:00
Pathological stage	
pTis	7
pTa	21
pT1	9
≥pT2	14
Grade	
Low grade	21
High grade	30

doi: 10.1111/j.1349-7006.2009.01379.x

of Health (Bethesda, MD, USA; available at http://rsb.info.nih.gov/ij/). All images were spatially calibrated for area measurements. Signal strength was recorded as electrons emitted per second of exposure. The area under the curve (AUC) was determined from plot profiles based on fluorescent signal strength and distribution in each individual bladder.

Statistical analysis. Data were statistically analyzed using the Student's *t*-test or non-parametric analysis Kruskal–Wallis test.[8,19,20] Results were considered significant if P was <0.05.

Results

Knockdown of syndecan-1 induced apoptosis in urothelial carcinoma cells. The effects of syndecan-1 gene silencing by siRNA were examined in human urothelial carcinoma cells. mRNA and protein expression was significantly reduced 72 h after siRNA transfection with an efficacy knockdown around 70–80% in the urothelial carcinoma cell lines UMUC2 and UMUC3 (Fig. 1a). Interestingly, knockdown of syndecan-1 induced apoptosis as determined by AV staining. The percentage of apoptosis in cells transfected with siRNA increased to 53.5% and 51.1% in UMUC2 and UMUC3 cells, respectively, whereas cell growth rates decreased to 60 and 75%, compared to cells transfected with control RNA (Fig. 1b,c). These results suggests that apoptosis was the main factor involved in syndecan-1 knockdown-induced cytotoxicity in urothelial carcinoma cells.

junB-mediated FLIP long signal is regulated by syndecan-1. To determine the mechanisms of apoptosis induced by syndecan-1 knockdown, we examined whether expression of several apoptotic or anti-apoptotic molecules including death receptors and Bcl-2 family members, were affected by manipulation of the syndecan-1 gene in urothelial carcinoma cells. As demonstrated in Figure 2(a), the long isoform of FLIP (FLIP long) was strongly down-regulated by syndecan-1 gene silencing in both UMUC2 and UMUC3 lines, but not other death receptor-related

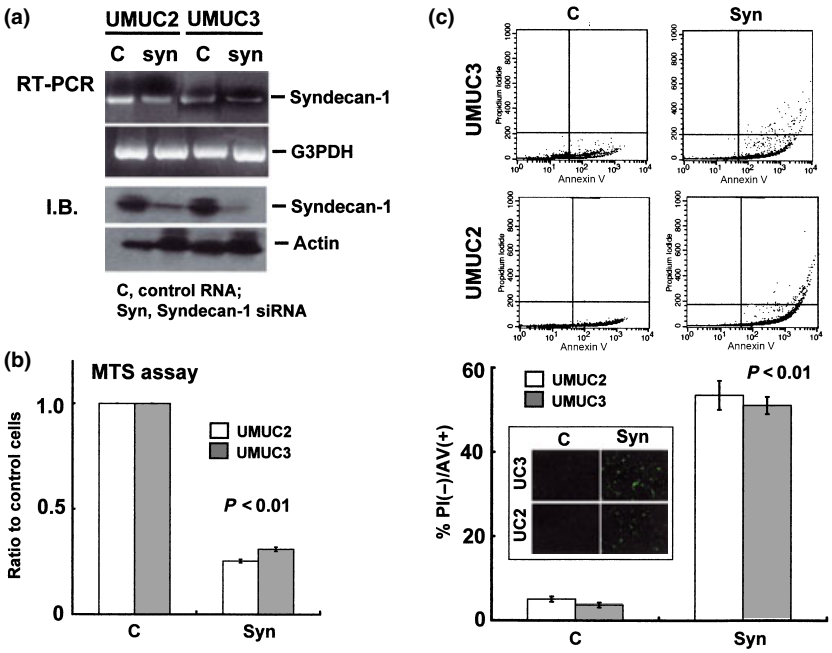

Fig. 1. Effect of syndecan-1 knockdown on cell survival in urothelial carcinoma cells. (a) UMUC2 and UMUC3 cells were transfected by control RNA or syndecan-1 siRNA (100 nM). mRNA and protein expression of syndecan-1 were examined by RT-PCR and Western blotting 72 h after cultivation. (b) Seventy-two hours after transfection, cell viability was assessed by MTS assay as described in the Materials and Methods. Values represent mean ratio to those after control RNA transfection. (c) Forty-eight hours after transfection, Annexin V and propidium iodide (PI) double staining were analyzed by flow cytometry (upper panels). Percentages of apoptotic cells (AV[+]/PI[−]) were measured by flow cytometry (lower panels). Inset photograph indicates cells positive for FITC-conjugated Annexin V (AV) using immunofluorescence microscopy. Each value is the mean ± SE. C, control RNA; Syn, syndecan-1 siRNA.

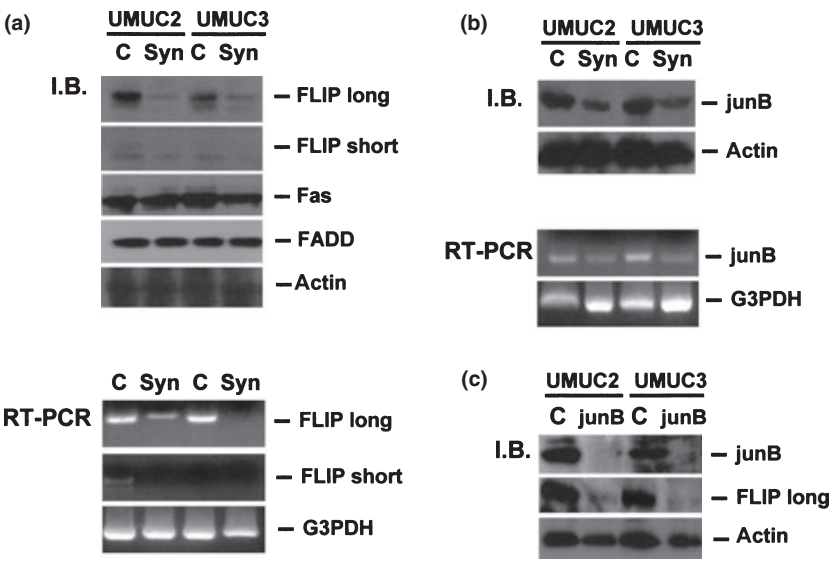

Fig. 2. junB and FLICE-inhibitory protein (FLIP long) are regulated by syndecan-1. (a,b) Seventy-two hours after control RNA or syndecan-1 siRNA transfection, expression of indicated molecules in UMUC2 and UMUC3 cells were examined by RT-PCR and Western blotting. (c) Cells were transfeced by junB siRNA, and protein expression of junB was examined by Western blotting after 72 h-cultivation. C, control RNA; junB, junB siRNA; Syn, syndecan-1 siRNA.

molecules such as Fas, FADD (Fig. 1a), and Death receptor 3 or 5 (data not shown). The short isoform of FLIP (FLIP short) was not significantly modulated after syndenca-1 siRNA transfection (Fig. 2a). Since a previous study reported that the activator protein (AP)-1 regulates transcriptional activity of the *FLIP* gene, we studied the role of the jun family members. The results showed that only junB expression was reduced in response to syndecan-1 knockdown; moreover, silencing the *junB* gene decreased FLIP long expression (Fig. 2b,c).

Downregulation of junB–FLIP long induced caspase-dependent apoptosis. We examined whether downregulation of junB or FLIP long induced apoptosis. As shown in Figure 3(a), not only did syndecan-1 induce apoptosis in UMUC2 and UMUC3 cells, so did FLIP long and junB silencing. Caspases 8 and 3 were cleaved by syndecan-1, FLIP long, or junB siRNA transfection, and apoptosis was significantly inhibited by treatment with the caspase 8 inhibitor z-IETD-fmk or the pan-caspase inhibitor z-vad-fmk (Fig. 3b).

***In vivo* growth of urothelial carcinoma is suppressed by syndecan-1 siRNA transfection in the orthotopic implant mouse model.** Figure 4(a) briefly illustrates the experimental protocol for the present study: KU-7 cells stably expressing RFP encoding vector were inoculated into the urinary bladder using transurethral catheter (Day 0). Seven days after inoculation (Day 7), we determined grafting to the bladder wall by fluorescence imaging and injected control RNA or syndecan-1 siRNA in the presence of atelocollagen into the urinary bladder. At Day 14, mice were sacrificed and tumor volume was estimated as described in the Materials and Methods. As shown in Figure 4(b,c), syndecan-1 down-regulation produced a ~threefold decrease in tumor area. Conventional histologic evaluation showed the same results: Control mice showed large tumors with cancer cells deeply infiltrating into the bladder wall, whereas only a few small cancerous foci located on surface of bladder tissue were observed in mice administered syndecan-1 siRNA in the presence of atelocollagen. Western blotting further confirmed that syndecan-1 and FLIP long expression was significantly decreased *in vivo* by this single injection of syndecan-1 siRNA *versus* control RNA, using human actin expression as a positive internal control (Fig. 5a,b). In addition, apoptotic cells determined by the TUNEL assay were much higher in tumor foci administered syndecan-1 siRNA than in those with control RNA injection. Taken together, syndecan-1 contributes to apoptosis resistance through junB–FLIP long signal in urothelial carcinoma cells.

Syndecan-1 is overexpressed in human urothelial carcinoma of the urinary bladder. Immunohistochemical analysis of syndecan-1 was performed in human bladder cancer specimens in order to establish the correlation of expression with pathological or clinical parameters including tumor grade and invasiveness. We examined surgical specimens consisting of low-grade/noninvasive, high-grade/invasive, and carcinoma *in situ* (CIS), all of which were diagnosed by two urologic pathologists. As shown in Figure 6(a), the percentages of immunopositive cells for

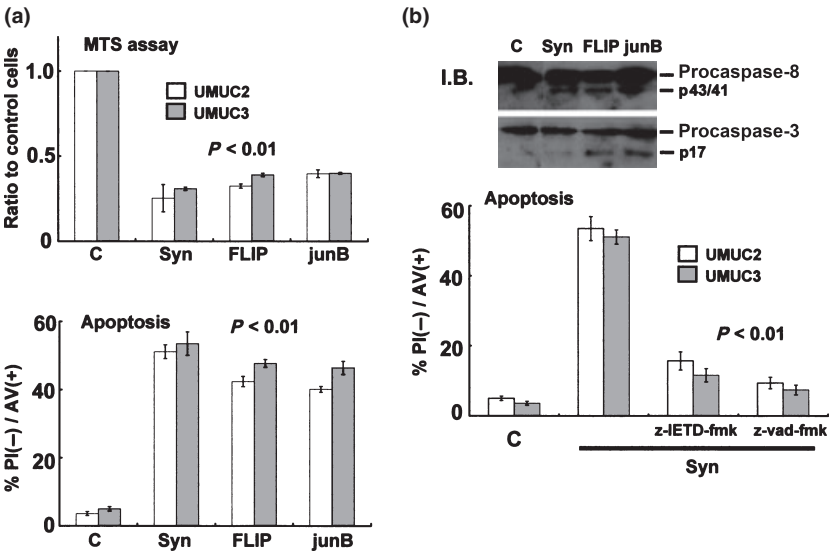

Fig. 3. Apoptosis induced by knockdown of syndecan-1, FLICE-inhibitory protein (FLIP long) or junB is dependent on caspase activation. (a) Seventy-two or 48 h after cultivation with control RNA, syndecan-1, FLIP long, or junB siRNA transfection, cell proliferation or apoptosis assays were performed as described in the Materials and Methods. Values for the MTS assay represent mean ratio to those after control RNA transfection (upper panel). Percentages of apoptotic cells (AV[+]/PI[−]) were measured by flow cytometry (lower panels). (b) Seventy-two hours after cultivation, pro-caspase-8 and -3 cleavage was analyzed by Western blotting (upper panel). Cells were transfected by control RNA or syndecan-1 siRNA, and pretreated with or without 25 μM of z-IETD-fmk or z-vad-fmk. Percentages of apoptotic cells were measured 48 h after cultivation (lower panels). C, control RNA; FLIP, FLIP long siRNA; junB, junB siRNA; Syn, syndecan-1 siRNA.

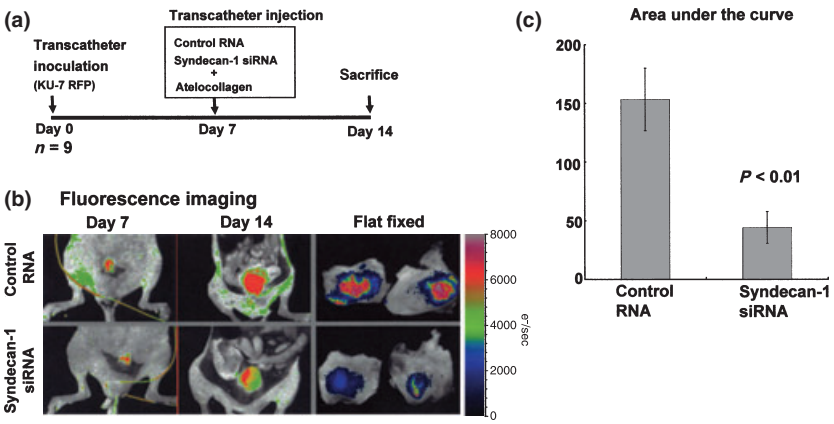

Fig. 4. Intravesical injection of syndecan-1 siRNA inhibits tumor growth *in vivo* in the mouse orthotopic bladder cancer implant model (1). (a) Diagrammatic experimental procedure. (b) Seven days after KU7/RFP cells were transplanted into the mouse bladder, atelocollagen with either syndecan-1 siRNA or control RNA was transurethrally instilled into the bladder lumen. Bladders were resected 7 days post-instillation, and *in situ* or *ex vivo* (after flat fixation) images were captured as described in the Materials and Methods. (c) Growth suppression in lesions treated with syndecan-1 siRNA/atelocollagen and control RNA/atelocollagen was compared in terms of tumor area measured by RFP expression. Each value is the mean ± SE.

doi: 10.1111/j.1349-7006.2009.01379.x

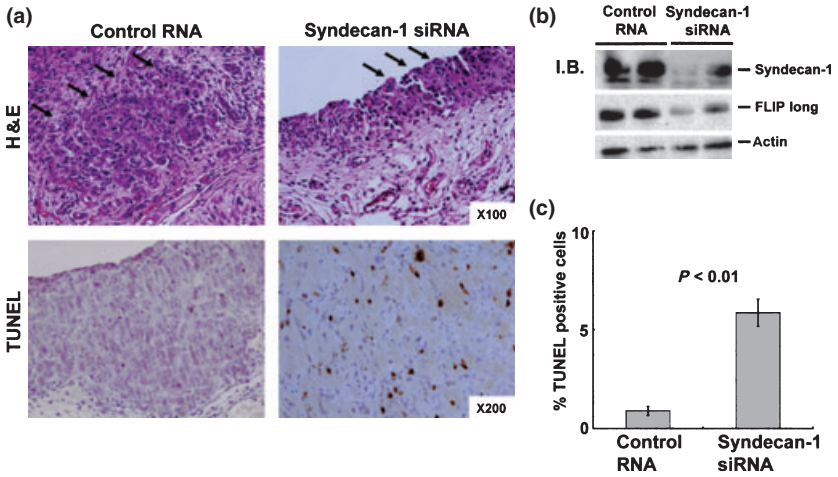

Fig. 5. Intravesical injection of syndecan-1 siRNA inhibits tumor growth *in vivo* in the mouse orthotopic bladder cancer implant model (2). (a) Cancerous tissues (arrows) and apoptotic cells were confirmed by corresponding H&E histologic sections (upper) and TUNEL staining (lower). (b) Bladder cancer samples were resected, lysed, and expression of syndecan-1 and FLIP long was determined by Western blot analysis. Expression of human actin was used as a loading control. (c) Indicates percentages of cells immunoreactive with TUNEL in resected bladder cancer specimens. The percentage was calculated per 1000 cells/high-power field. Each value is the mean ± SE.

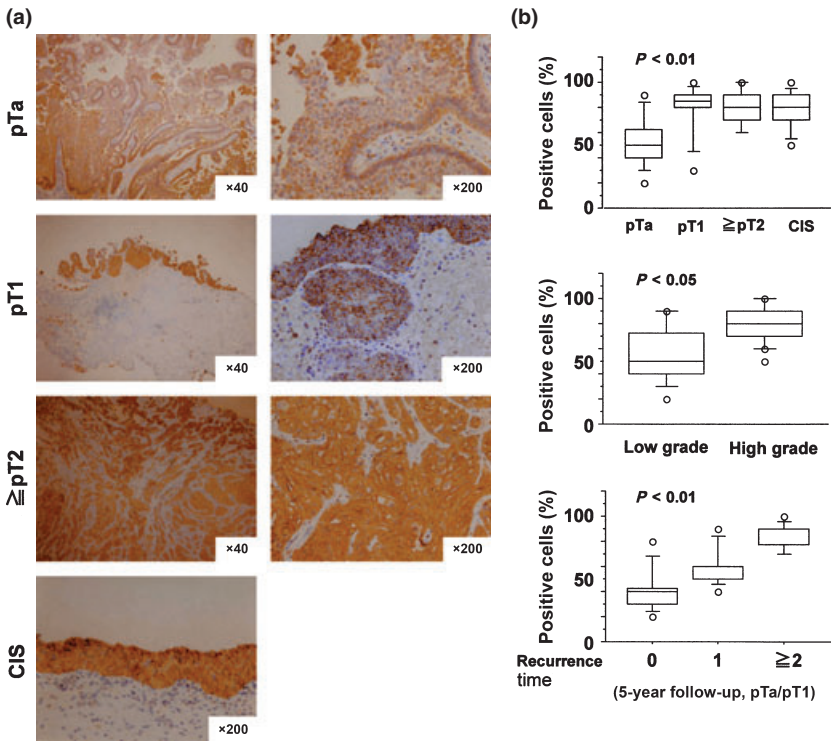

Fig. 6. Immunohistochemical analysis of syndecan-1 in human urothelial bladder carcinomas indicates a correlation with tumor grade. (a) Immunohistochemistry for syndecan-1 expression was performed on representative samples of each group. The percentage of immunopositive cells was calculated per 1000 cells/high-power field. As can be seen, there seems to be a positive correlation between the percentages of syndecan-1 immunopositive cells and tumor grade, T-stage, or times of tumor recurrence (pTa/pT1, n = 38) within 5 years. Each value is the mean ± SE.

syndecan-1 were much higher in high-grade urothelial carcinomas, including CIS, with both minimal (pT1) and wide invasion (≥pT2) than in low-grade (G1 and G2) lesions with a noninvasive phenotype (pT_a). Interestingly, percentages of positive cells for syndecan-1 at initial diagnosis of pTa/pT1 cancers (n = 38) closely correlated to time of recurrence within 5 years, suggesting immunoreactivity for syndecan-1 may be a useful marker for predicting urothelial carcinoma progression.

Discussion

We demonstrated here for the first time that syndecan-1 plays an important role in cell survival via junB-dependent FLIP long signal in human urothelial carcinoma *in vitro* and *in vivo* experiments.[7,22] To date, several reports have demonstrated the mechanisms by which syndecan-1 affects the progression of human cancer. More recently, syndecan-1 has been shown to interact with the alpha(v)beta(3) and alpha(v)beta(5) integrins, resulting in enhanced angiogenesis and tumor development of human breast cancer, which could be blocked by a peptide inhibitor called synstatin. [23] Unlike these reports targeting the role of syndecan-1 as matrix protein receptor, the current study examined its effects on apoptosis in urothelial carcinoma cells: syndecan-1 stabilizes FLIP long through junB, closely associated with resistance to apoptosis. It is generally accepted that silencing of FLIP long alone cannot induce apoptosis, but DISC plus FLIP long was constitutively formed in urothelial carcinoma cell lines currently used (data not shown), and a reduction of FLIP could directly lead to activation of DISC and subsequent caspase 8 cleavage. This scenario is supported by other investigations demonstrating that FLIP long prevents spontaneous apoptosis dependent on Death receptor 5 through the formation of the apoptosis inhibitory complex (DISC + FLIP long) in a breast cancer cell line.[24] FLIP inhibits apoptosis involving not only Fas but also other kinds of death-receptors [25]; therefore, syndecan-1 provides the best target for successful treatment using a death-receptor ligand. Another example is tumor necrosis factor–related apoptosis-inducing ligand (TRAIL), which can selectively induce apoptosis in urothelial carcinoma cells while sparing normal cells. On the other hand,

transient overexpression of FLIP has been reported to bind to Raf-1 and activate extracellular signal regulating kinase and nuclear factor-kappa B. Moreover, we have previously found that FLIP stimulates prostate cancer cell survival by stabilizing beta-catenin.[26,27] These investigations raise the possibility that overexpression of syndecan-1 may directly enhance cell survival. JunB is one of the jun family members and is composed of AP-1 homo- or heterodimers.[28] Mostly, junB negatively regulates the transforming activity of c-*jun* by forming heterodimers,[29] and c-*jun*-c-*Fos* was recently reported to negatively regulate FLIP transcription by which MG132 could sensitize prostate cancer cells to TRAIL-induced apoptosis.[30] However, neither binding of junB to promter region nor formation of heterodimers of junB-c-*jun* or junB-c-*Fos* was observed in the present study (data not shown). Other molecules might intervene with the interaction between junB and FLIP long transcription.

In the orthotropic implantation model, we found that a single injection of syndecan-1 siRNA, in the presence of atelocollagen, strongly down-regulated syndecan-1 and FLIP long protein expression, resulting in a reduction of tumor volume. The results clearly showed that syndecan-1-mediated cell survival signals actually function *in vivo*, and that syndecan-1 targeting therapy for urinary bladder cancer could be a more useful therapeutic tool.[8]

Immunohistochemical analyses on human bladder cancer samples suggest that increased expression of syndecan-1 contributes to signal activation early in the development of urothelial carcinoma and is linked to the change from a noninvasive to an invasive bladder cancer. Other studies posit that immunoprofiling of syndecna-1, as well as of TP53, will provide more reliable information for bladder cancer prognosis.[31] One more important and novel finding is that syndecan-1 is a useful marker for prediction of bladder cancer recurrence. Post-operative examination or treatment effects should be carefully performed in cases of urothelial carcinomas with high expression of syndecan-1 at initial diagnosis.

In summary, syndecan-1 is up-regulated in urothelial carcinomas, particularly in high-grade/invasive cancer and it positively affects cancer cell survival via junB–FLIP long signals involving not only resistance to apoptosis but also enhancement of cell growth. Silencing syndecan-1 by siRNA transfection suppressed the malignant potential in *in vitro* and *in vivo* studies; moreover, transurethral injection of siRNA combined with atelocollagen may be an effective delivery system to achieve successful down-regulation of the gene and provide a new strategy for the treatment of advanced urothelial carcinoma.

Acknowledgment

This research was supported in part by a Grant-in-Aid from the Ministry of Education, Culture, Sports, Science and Technology of Japan (no. 19390104).

References

1 Bernfield M, Gotte M, Park PW *et al.* Functions of cell surface heparan sulfate proteoglycans. *Annu Rev Biochem* 1999; **68**: 729–77.
2 Dhodapkar MV, Abe E, Theus A *et al.* Syndecan-1 is a multifunctional regulator of myeloma pathobiology: control of tumor cell survival, growth, and bone cell differentiation. *Blood* 1998; **91**: 2679–88.
3 Wijdenes J, Vooijs WC, Clement C *et al.* A plasmocyte selective monoclonal antibody (B-B4) recognizes syndecan-1. *Br J Haematol* 1996; **94**: 318–23.
4 Mahtouk K, Cremer FW, Reme T *et al.* Heparan sulphate proteoglycans are essential for the myeloma cell growth activity of EGF-family ligands in multiple myeloma. *Oncogene* 2006; **25**: 7180–91.
5 Derksen PW, Keehnen RM, Evers LM, Van Oers MH, Spaargaren M, Pals ST. Cell surface proteoglycan syndecan-1 mediates hepatocyte growth factor binding and promotes Met signaling in multiple myeloma. *Blood* 2002; **99**: 1405–10.
6 Yang Y, MacLeod V, Dai Y *et al.* The syndecan-1 heparan sulfate proteoglycan is a viable target for myeloma therapy. *Blood* 2007; **110**: 2041–8.
7 Nikolova V, Koo CY, Ibrahim SA *et al.* Differential roles for membrane-bound and soluble syndecan-1 (CD138) in breast cancer progression. *Carcinogenesis* 2009; **30**: 397–407.
8 Shimada K, Nakamura M, Anai S *et al.* A novel human AlkB homologue, ALKBH8, contributes to human bladder cancer progression. *Cancer Res* 2009; **69**: 3157–64.
9 Hanahan D, Weinberg RA. The hallmarks of cancer. *Cell* 2000; **100**: 57–70.
10 Wu XR. Urothelial tumorigenesis: a tale of divergent pathways. *Nat Rev* 2005; **5**: 713–25.
11 Jebar AH, Hurst CD, Tomlinson DC, Johnston C, Taylor CF, Knowles MA. FGFR3 and Ras gene mutations are mutually exclusive genetic events in urothelial cell carcinoma. *Oncogene* 2005; **24**: 5218–25.
12 Mhawech-Fauceglia P, Cheney RT, Schwaller J. Genetic alterations in urothelial bladder carcinoma: an updated review. *Cancer* 2006; **106**: 1205–16.
13 Liebert M, Seigne J. Characteristics of invasive bladder cancers: histological and molecular markers. *Semin Urol Oncol* 1996; **14**: 62–72.
14 Shimada K, Nakamura M, Ishida E *et al.* C-Jun NH2 terminal kinase activation and decreased expression of mitogen-activated protein kinase phosphatase-1 play important roles in invasion and angiogenesis of urothelial carcinomas. *Am J Pathol* 2007; **171**: 1003–12.
15 Shimada K, Nakamura M, Ishida E, Konishi N. Urothelial carcinoma with plasmacytoid variants producing both human chorionic gonadotropin and carbohydrate antigen 19-9. *Urology* 2006; **68**: 891–e7.
16 Nigwekar P, Tamboli P, Amin MB, Osunkoya AO, Ben-Dor D, Amin MB. Plasmacytoid urothelial carcinoma: detailed analysis of morphology with clinicopathologic correlation in 17 cases. *Am J Surg Pathol* 2009; **33**: 417–24.
17 Shimada K, Nakamura M, Konishi N. A case of urothelial carcinoma with triple variants featuring nested, plasmacytoid, and lipoid cell morphology. *Diagn Cytopathol* 2009; **37**: 272–6.
18 Sabichi A, Keyhani A, Tanaka N *et al.* Characterization of a panel of cell lines derived from urothelial neoplasms: genetic alterations, growth in vivo and the relationship of adenoviral mediated gene transfer to coxsackie adenovirus receptor expression. *J Urol* 2006; **175**: 1133–7.
19 Shimada K, Matsuyoshi S, Nakamura M, Ishida E, Konishi N. Phosphorylation status of Fas-associated death domain-containing protein (FADD) is associated with prostate cancer progression. *J Pathol* 2005; **206**: 423–32.
20 Konishi N, Nakamura M, Kishi M, Nishimine M, Ishida E, Shimada K. Heterogeneous methylation and deletion patterns of the INK4a/ARF locus within prostate carcinomas. *Am J Pathol* 2002; **160**: 1207–14.
21 De Velasco MA, Tanaka M, Anai S, Tomioka A, Nishio K, Uemura H. GFP image analysis in the mouse orthotopic bladder cancer model. *Oncol Rep* 2008; **20**: 543–7.
22 Su G, Blaine SA, Qiao D, Friedl A. Membrane type 1 matrix metalloproteinase-mediated stromal syndecan-1 shedding stimulates breast carcinoma cell proliferation. *Cancer Res* 2008; **68**: 9558–65.
23 Beauvais DM, Ell BJ, McWhorter AR, Rapraeger AC. Syndecan-1 regulates alphavbeta3 and alphavbeta5 integrin activation during angiogenesis and is blocked by synstatin, a novel peptide inhibitor. *J Exp Med* 2009; **206**: 691–705.
24 Day TW, Huang S, Safa AR. c-FLIP knockdown induces ligand-independent DR5-, FADD-, caspase-8-, and caspase-9-dependent apoptosis in breast cancer cells. *Biochem Pharmacol* 2008; **76**: 1694–704.
25 Irmler M, Thome M, Hahne M *et al.* Inhibition of death receptor signals by cellular FLIP. *Nature* 1997; **388**: 190–5.
26 Kataoka T, Budd RC, Holler N *et al.* The caspase-8 inhibitor FLIP promotes activation of NF-kappaB and Erk signaling pathways. *Curr Biol* 2000; **10**: 640–8.
27 Shimada K, Nakamura M, Matsuyoshi S, Ishida E, Konishi N. Specific positive and negative effects of FLIP on cell survival in human prostate cancer. *Carcinogenesis* 2006; **27**: 1349–57.
28 Shaulian E, Karin M. AP-1 in cell proliferation and survival. *Oncogene* 2001; **20**: 2390–400.
29 Shaulian E, Karin M. AP-1 as a regulator of cell life and death. *Nat Cell Biol* 2002; **4**: E131–6.
30 Li W, Zhang X, Olumi AF. MG-132 sensitizes TRAIL-resistant prostate cancer cells by activating c-Fos/c-Jun heterodimers and repressing c-FLIP(L). *Cancer Res* 2007; **67**: 2247–55.
31 Sauter G, Moch H, Mihatsch MJ, Gasser TC. Molecular cytogenetics of bladder cancer progression. *Eur Urol* 1998; **33** (Suppl 4): 9–10.

doi: 10.1111/j.1349-7006.2009.01379.x